Seismic data regularization with the anti-alias anti-leakage Fourier transform

Michel Schonewille,[1] Andreas Klaedtke,[1] Alan Vigner,[1] John Brittan[1*] and Tony Martin[1] present a solution to a problem with regularly sampled data found in the use of the anti-alias anti-leakage Fourier transform (ALFT).

The anti-leakage Fourier transform (ALFT) is a regularization method using an iterative procedure for computing the spectrum of irregularly sampled data. For each iteration a discrete Fourier transform is performed. Then, the maximum Fourier component is selected and transformed back to the irregular grid. The component is subtracted from the input data, and the result is used in the next iteration. For irregularly sampled data, the ALFT can handle very steep dips, but for regularly sampled data, the aliased Fourier components of a certain event have the same amplitude as the true component. Consequently, the aliased components may be estimated, and the event is not properly reconstructed. In practice, results can also be degraded for situations where the sampling is close to regular. In this article, we show the results of using the un-aliased lower frequencies to provide spectral weights for the higher frequencies. This helps to avoid selection of the aliased component. It is shown on 2D synthetic and 3D field data that the method can give a significant improvement for data with steeply dipping events.

Background

Seismic datasets are generally irregularly sampled in inline midpoint, cross-line midpoints, offset and azimuth. This irregular sampling can give lead to both poor levels of repeatability between 4D surveys (Eiken et al., 1999) and artifacts in pre-stack imaging (see, for example, Canning and Gardner, 1996). Irregular sampling can also limit the effectiveness of high-end 3D demultiple and imaging algorithms such as 3D SRME and wave-equation pre-stack depth migration (PSDM). To overcome this issue, it is common in seismic data processing to use regularization and interpolation. Although precise definitions vary, the process of regularization is usually described as being that which transfers samples from their irregular recorded location to locations on a regular grid. Interpolation processes are used to fill in any samples in that regular grid that are missing (extrapolation is generally held to be a process related to interpolation, albeit with its own special difficulties). In this article we discuss technology that can be used to undertake these processes, and, in particular, a method for both interpolating and regularizing aliased datasets using the anti-leakage Fourier transform (ALFT).

Figure 1 schematically describes the main areas of seismic processing in which interpolation and regularization have an impact although it is probably true that no significant seismic dataset is processed without the application of at least one interpolation and/or regularization method.

Different methods of regularization and interpolation

There are several methods for regularization and interpolation, and these have different characteristics. A comparison of some of the characteristics is shown in Table 1. Binning, either static or flex(ible), is based on simply choosing a trace with certain characteristics and moving it (without

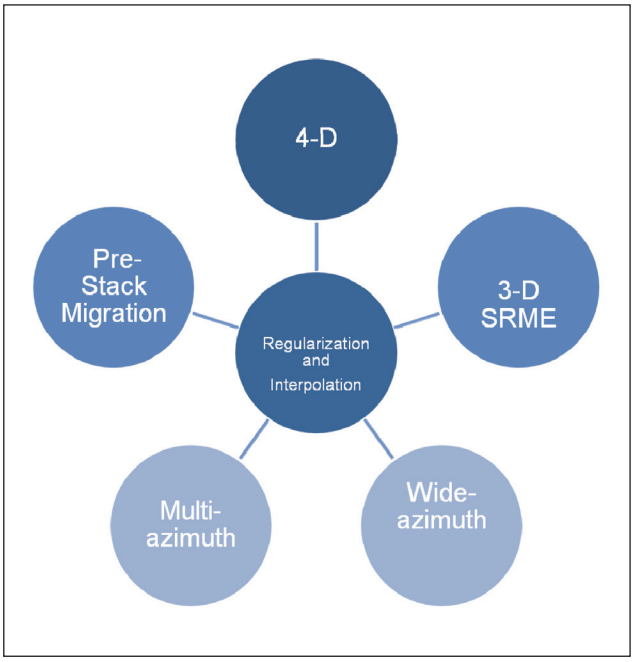

Figure 1 *Schematic diagram showing the areas of major use of regularization and interpolation.*

[1] *Petroleum Geo-Services, Weybridge, Surrey, KT13 0NY, UK.*
** Corresponding author, E-mail: john.brittan@pgs.com*

Method	Assumptions	Interpolation beyond Aliasing	Characteristics
(Flex)-Binning	Local 1-D assumption	No	Very cheap
DMO/DMO^{-1} AMO	Model needed	No	Variable speed. Can be expensive.
f-k/*f-x*/*f-x-y* Interpolation	Limited number of dips present in data. Regular spatial sampling	Yes	Cheap. Not optimal for larger gaps.
Radon transform Interpolation	Limited number of dips present in data	Yes	Cheap. Handles conflicting dips & large gaps
Fourier regularization	Band-limited data	Yes	More costly.

Table 1 *Comparison of characteristics of interpolation and regularization technology.*

adjusting the trace data itself) to a given bin location. The choice of trace can be made based on one or a combination of characteristics (e.g. in 4D processing it is common to choose the trace from monitor survey with the minimum value of $\Delta s+\Delta r$ where Δs is the distance of the monitor source location from the base source location and Δr is the distance of the monitor receiver location from the base receiver location).

Flex binning was once the main method in the seismic processing industry to handle empty bins, but nowadays it is much more common to use some form of amplitude and dip-friendly interpolation (for example, a Radon transform-based interpolation). Pre-stack partial migration (DMO, inverse DMO and, in particular, AMO) has also been commonly applied as a regularization methodology and can be used if a correction of azimuths is needed. The main drawback to such methods is a tendency towards operator instability at wide azimuths and near offsets. *f-x* and *f-x-y* techniques are typically used to interpolate regularly sampled data to a finer grid. However, in this article we will concentrate on a Fourier regularization method using the ALFT.

The anti-leakage Fourier transform (ALFT) utilized is one of a class of algorithms knows as Fourier regularization methods. The general principle of Fourier regularization is to compute the spectrum of irregularly sampled data, and then use an inverse transform to reconstruct data at new locations (Figure 2). The inverse transform is straightforward, and can be done with a standard inverse discrete Fourier transform (DFT) or inverse fast Fourier transform (FFT). However, the direct forward transform using a DFT is not optimal, and suffers from 'spectral leakage' in the Fourier domain. This spectral leakage can be understood by realizing that a sampled signal can be seen as a continuous signal multiplied by an impulse train. This multiplication is equivalent to convolution in the Fourier domain with the Fourier transform of the pulse train.

In the case of irregular sampling, this function typically has a strong peak at zero frequency (DC component), but also non-zero amplitudes at non-zero frequencies. The convolution means that energy at a certain frequency 'leaks' to adjacent frequencies. If the spectrum is then used to reconstruct data at new locations, the results are not optimal (Figure 3).

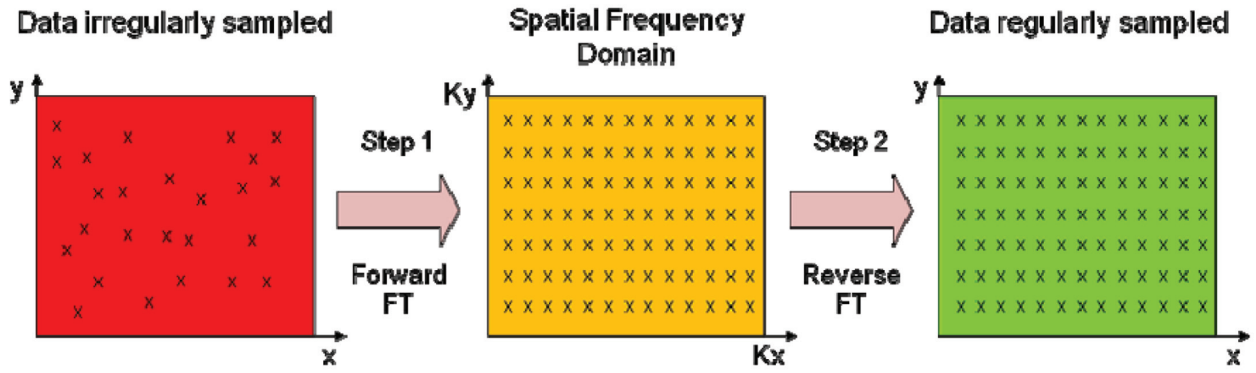

Figure 2 *The general principle of Fourier regularization.*

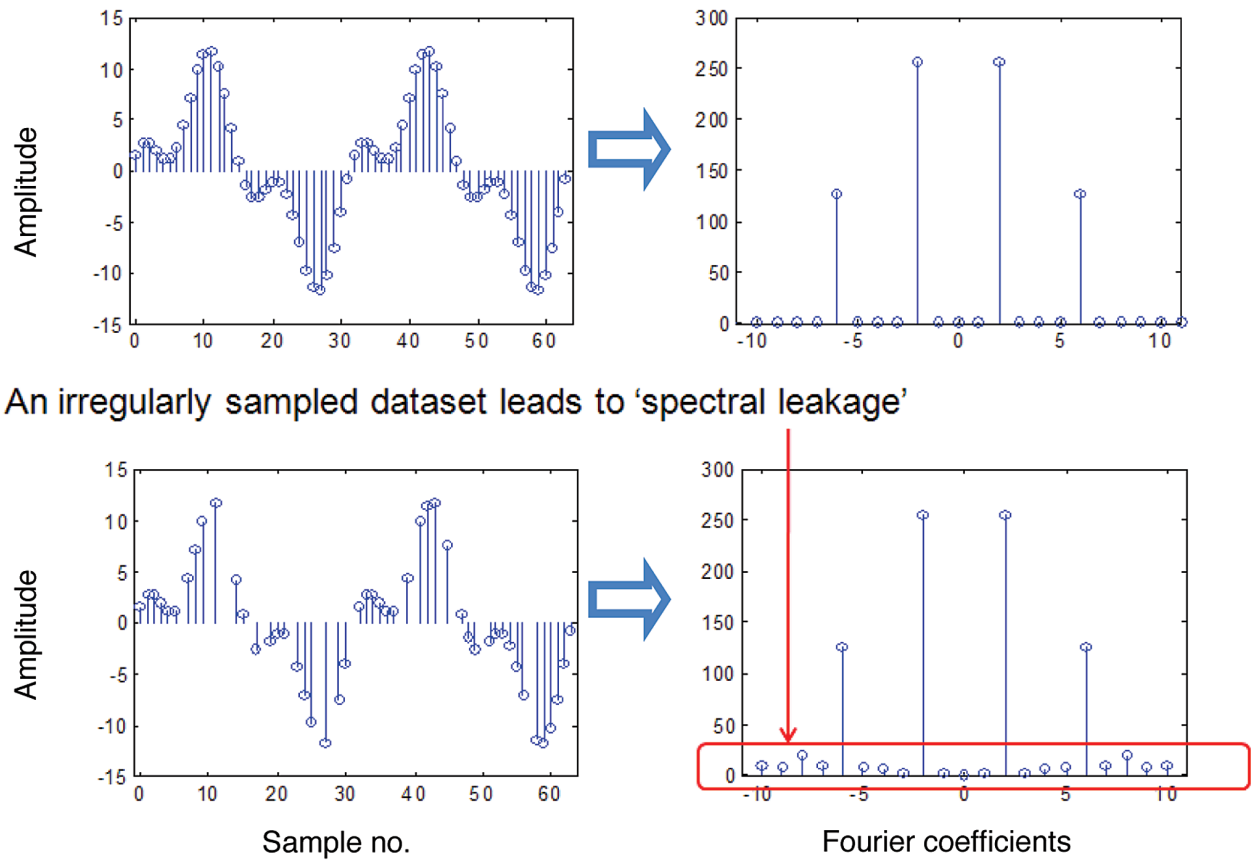

Figure 3 *Taking a direct forward transform from the time domain (left) to the Fourier domain (right) of a regularly sampled dataset (top) and an irregularly sampled dataset (bottom) leads to different results. The irregularly sampled dataset suffers from spectral leakage in the Fourier domain.*

Fourier regularization methods, therefore, should not use the DFT to do the forward transform. A least-squares estimation of Fourier components would be an example of a better option (e.g., Duijndam et al., 1999). As long as the data are band-limited and sufficiently well sampled, the least squares Fourier regularization (and other methods, including the ALFT) can completely eliminate spectral leakage. In practice, however, seismic data are often also sparsely sampled, and can show large gaps in the sampling. In these situations a standard least-squares estimation can become poorly determined, and the estimation of the spectrum sub-optimal. Several methods have been proposed to improve on the standard least-squares method, such as the high-resolution transforms (see Sacchi and Ulrych, 1996, Zwartjes and Sacchi, 2007), MWNI (Liu and Sacchi, 2004), POCS (Abma and Kabir, 2006), and the ALFT (Xu et al., 2004 and 2005). The standard ALFT can handle sparsely sampled data to some extent, but interestingly, the performance can degrade for data with sampling that only shows limited irregularities. In this article we introduce an improved version of the standard ALFT to minimize the spectral leakage in the forward transform.

Anti-leakage Fourier transform (ALFT)

Although the actual implementation used is more computationally efficient, in principle, for each iteration, the following steps are done (see Xu et al., 2004 for more details and Figure 4 for an example):

1. Compute the DFT of the input data.
2. Select the strongest Fourier component.
3. Add this component to the 'estimated spectrum'
4. Inverse DFT of this component to the original grid.
5. Subtract the component from the input data.

The last step provides the input data for the next iteration. When sufficient iterations have been done, the estimated spectrum can be used to create data at new locations using an inverse DFT or, in case of a regular output grid, an inverse FFT. Note that due to spectral leakage of other components, the initial estimate of the strongest component (and other components) may not be exact, and the same component can be chosen again in later iterations.

As mentioned before, the ALFT can handle sparsely sampled data, but the performance can degrade for data that is close to regular. To explain this, consider the example in Figure 5 which shows the spectrum of a

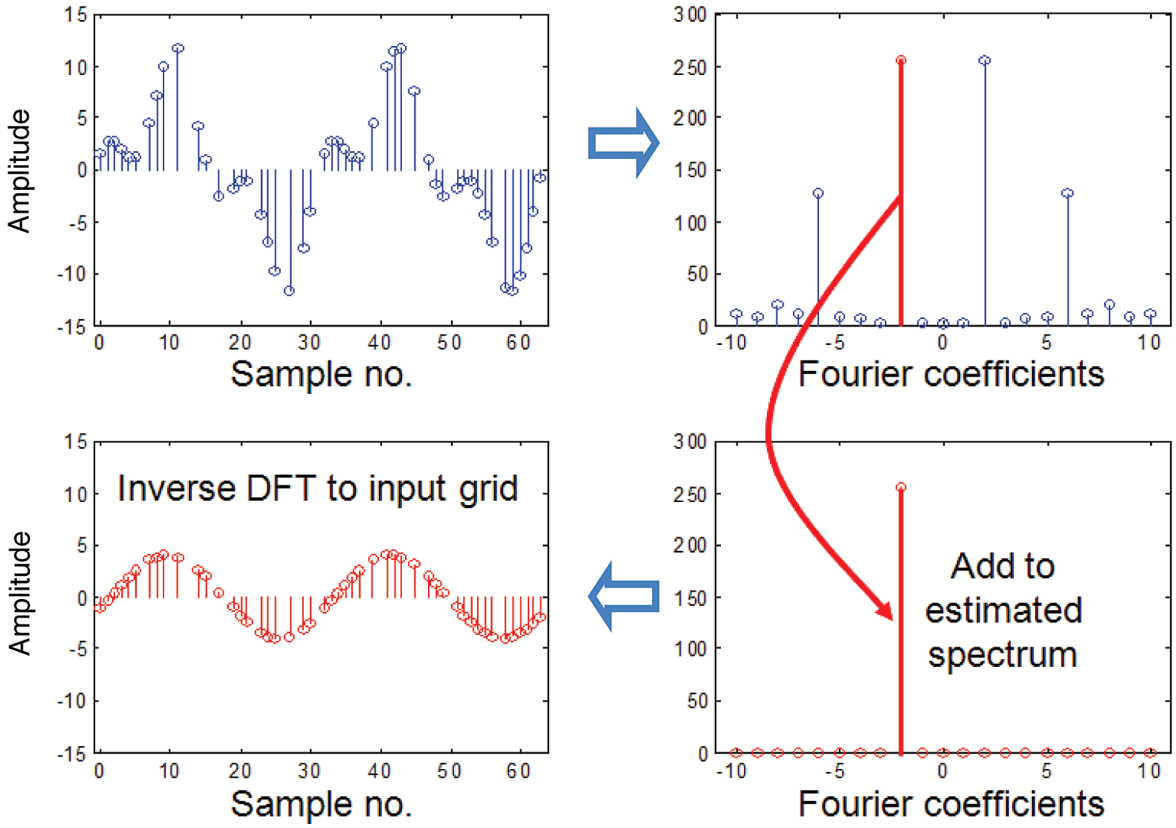

Figure 4 *A schematic representation of a single iteration of the anti-leakage Fourier transform (ALFT). Starting at the top left, the DFT of the input data is calculated (top right); the maximum of the Fourier coefficients is chosen and added to the estimated output spectrum (bottom right); this coefficient is then taken through an inverse DFT to the input grid (bottom left) and subtracted from the input data.*

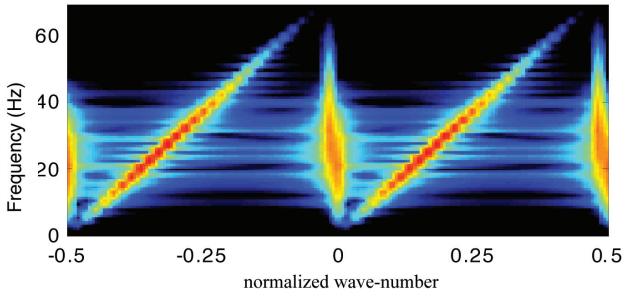

Figure 5 *Spectrum of a regularly sampled data set with two events computed over a twice as large bandwidth as normal.*

simple dataset with two dipping layers. Due to the sparse sampling, relative to the bandwidth of the data, aliasing is visible. Note that a normal FK-spectrum would only show the spectrum up to a normalized wave-number of 0.25 (in this figure), but when using a DFT, a larger k-range can be specified. It can be seen that the spectrum is repeated. A regularly sampled signal can be seen as a continuous signal that is multiplied by an impulse train with sampling interval Δx. This is equivalent to convolution in the Fourier domain with a pulse train with sampling interval $1/\Delta x$. As a result, the true spectrum of the signal is repeated, in principle, an infinite number of times. This also means that the aliased spectra are identical and, more importantly, as strong in amplitude as the true spectrum. Consequently, when the ALFT selects the strongest component, it may well be the aliased component instead of the true component in a practical computer implementation. This would mean that the event is not reconstructed well at new locations.

Anti-alias anti-leakage Fourier transform

The following method can be used to improve the handling of aliased energy (Schonewille et al., 2009):

1. Compute the spectrum for the un-aliased frequencies using the standard ALFT.
2. Extrapolate the absolute spectrum to higher frequencies and higher *k*-values to obtain weights for the higher frequencies.
3. Compute the ALFT for the aliased frequencies, but select the maximum weighted component.

The weights are derived from the smoothed absolute spectrum (Figure 6). For the higher frequencies, the weights increase the amplitudes of the true events, and consequently, the true event will be stronger than the aliased components, and be selected

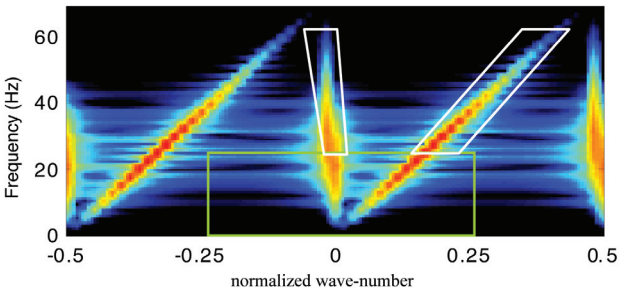

Figure 6 *The weights are computed at unaliased frequencies (in the green box) and applied to the higher frequencies. The amplitudes of the events in the white polygons will be increased.*

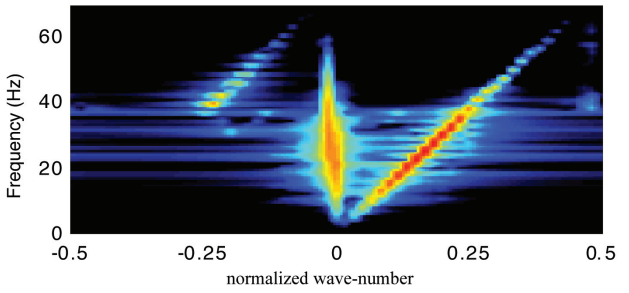

Figure 8 *Spectrum of the data in Figure 5 estimated with the standard ALFT with variable bandwidth, which is smaller for lower frequencies.*

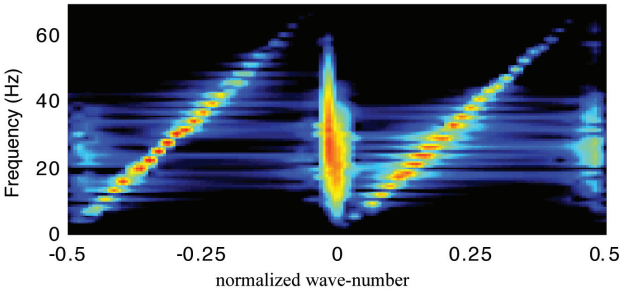

Figure 7 *Spectrum of the data in Figure 5 estimated using the standard ALFT.*

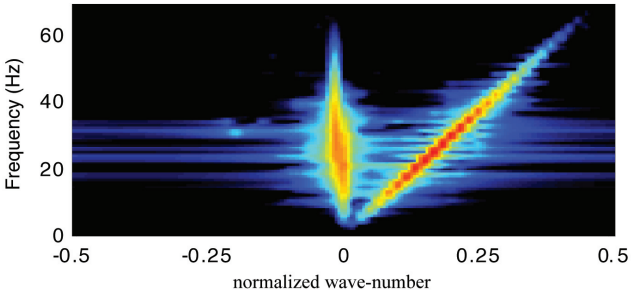

Figure 9 *Spectrum of the data in Figure 5 estimated with the anti-alias ALFT.*

by the ALFT. Note that the un-weighted component is added to the estimated spectrum. The improvement the anti-alias ALFT gives over the standard ALFT can be illustrated using synthetic data.

As an illustration, in Figure 7 the spectrum of Figure 5 estimated with a standard ALFT is shown. The implementation of the ALFT used in this example works on each frequency slice using the full bandwidth. It will be clear that a spectrum like this cannot provide a satisfactory interpolation.

A significant improvement can be obtained with the standard ALFT by using a variable bandwidth, which is smaller for lower frequencies. The result of this method is shown in Figure 8. Note that this method clearly cannot remove the problems at higher frequencies.

In Figure 9, the results of the anti-alias ALFT are shown. In this case the estimated spectrum is close to the desired spectrum.

The data after reconstruction onto a finer grid using the spectra in Figure 8 and 9, as well as the difference with the ideal data, are shown in Figure 10. The anti-alias method clearly improves the reconstruction of the high frequencies for the steepest event. The stronger the aliasing in the data, the bigger these differences will be. Note that both methods show some edge effects, but these can in practice be reduced, for example by windowing,

Data examples

In Figures 11-14, a 3D field data example is given. The data volume was processed in overlapping 3D windows of 20 cross-lines by 40 inlines, and 32 time samples. The exact midpoints are used, and no duplicate trace rejection is done. The trace weighting scheme is based on Voronoi tessellation.

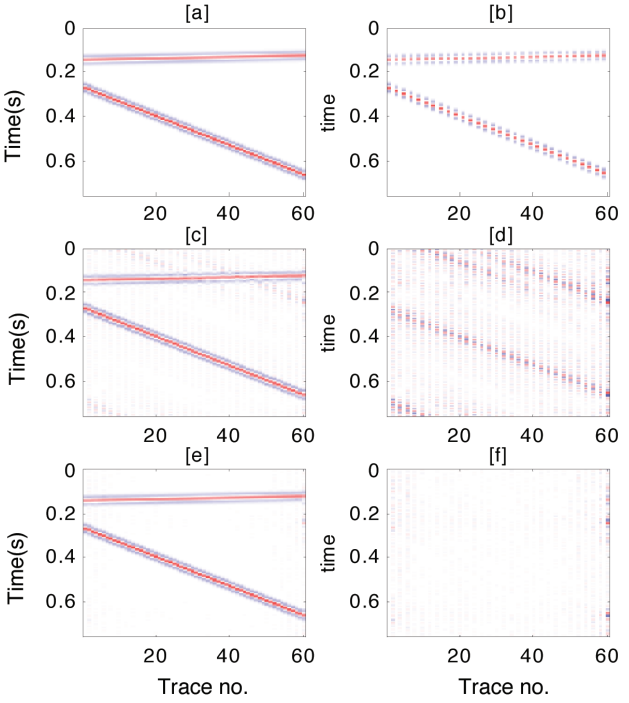

Figure 10 *a) Ideal data; b) Input data; c) data reconstructed with the standard ALFT with variable bandwidth; d) Difference between c and a; e) data reconstructed with anti-alias ALFT; f) Difference between e and a.*

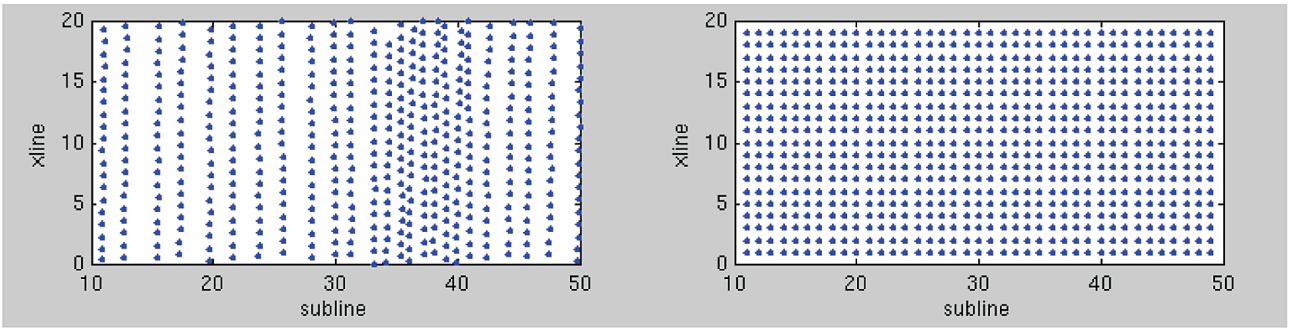

Figure 11 *The midpoint sampling before (left) and after (right) regularization. The inline and cross-line spacing is 12.5 m.*

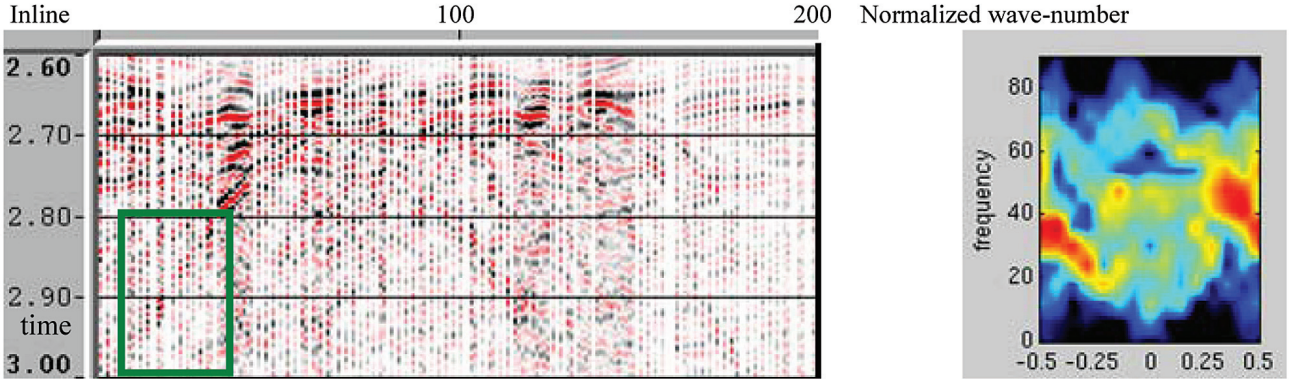

Figure 12 *One cross-line section of 3-D input data (left) and f-k spectrum of the diffraction event in the green box (right).*

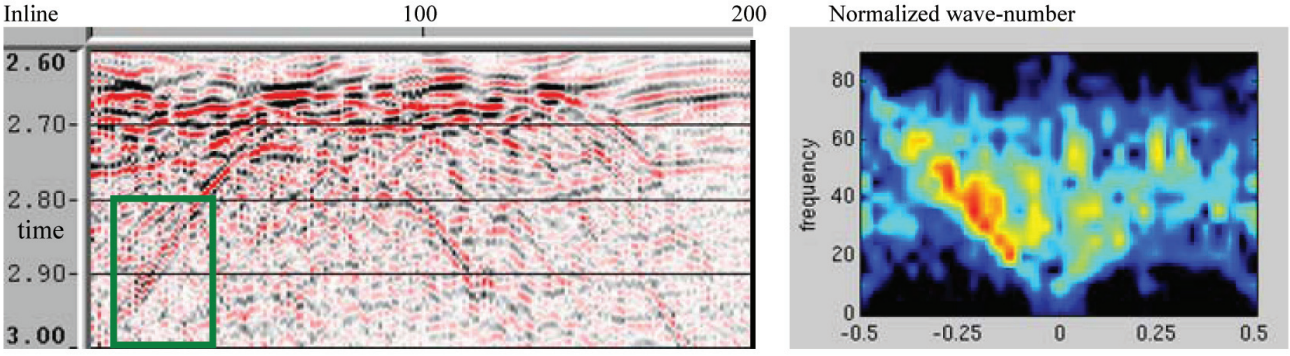

Figure 13 *One cross-line section after full bandwidth ALFT (left) and f-k spectrum of data in green box (right).*

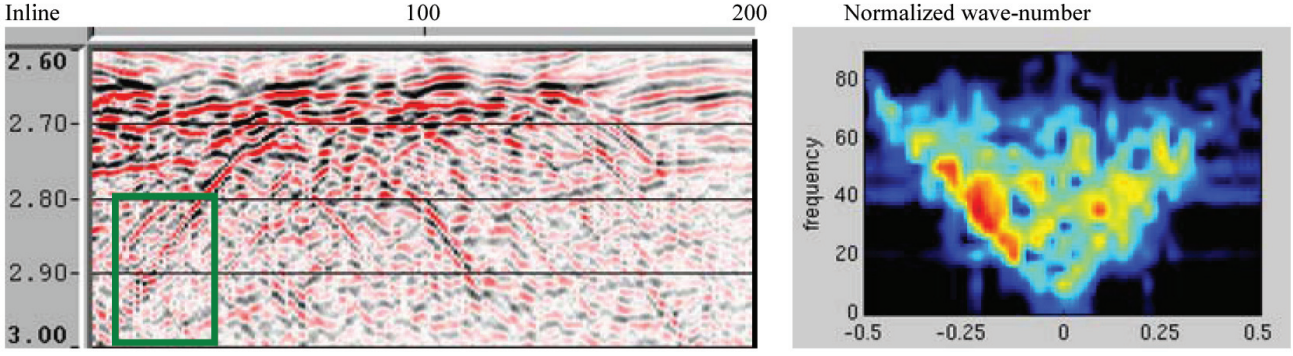

Figure 14 *One cross-line section of the data after variable bandwidth ALFT (left) and FK spectrum of data in green box (right).*

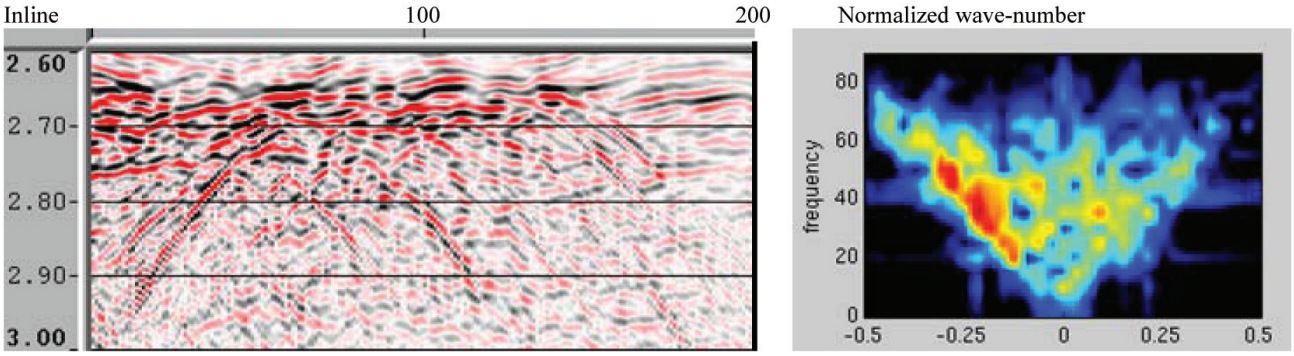

Figure 15 *One cross-line section of the data after anti-alias ALFT (left) and f-k spectrum of data in green box (right). The anti-alias ALFT combines the advantages of a variable bandwidth (as shown in Figure 14) with further de-aliasing of the higher frequencies, leading to an excellent reconstruction of the steeply dipping events in this complex and sparsely sampled area.*

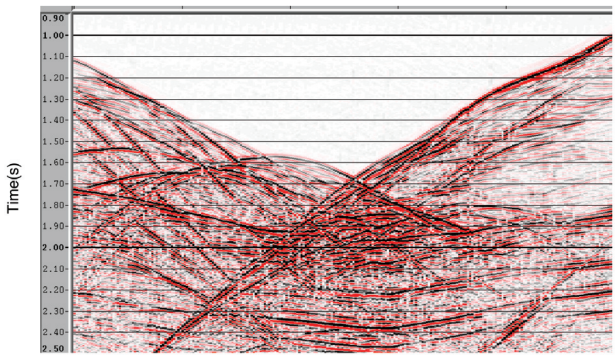

Figure 16 *An example inline from a second marine 3D dataset illustrating the complexity of the dataset to be regularized.*

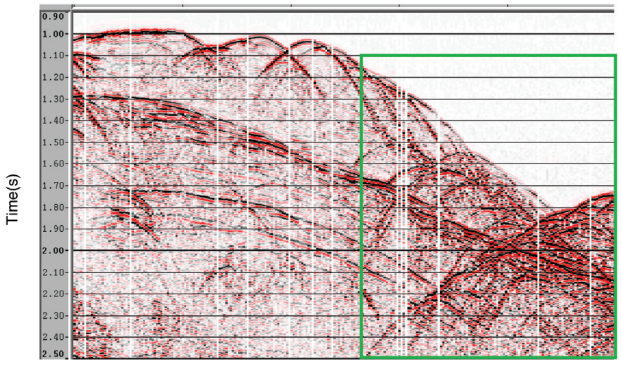

Figure 17 *A cross-line section from the second example dataset showing the aliasing present in many of the dipping events. Figures 18 and 19 show data in the area bounded by the green box.*

The data are from the Faeroes-Shetland basin, and for this example an area with particularly steeply dipping diffraction events is selected.

In Figure 11, the sampling before and after regularization is shown. For most of the data, the output cross-line sampling is twice as dense as the input sampling.

In Figure 12, part of the input data is shown with a complex area of steeply dipping diffraction events highlighted. (For display only, static binning was applied, and zero traces are shown for empty bins). The *f-k* spectrum (using live traces only) on the right is plotted twice as narrow as the other spectra since the average trace spacing is twice as large as for the regularized data.

Figure 13 shows the results of the ALFT with a full spatial bandwidth (on the output grid) for all frequencies. The presence of aliased energy is obvious, in particular, in the spectrum at normalized wavenumbers +/- 0.5 which leads to jitter for some events. The steeply dipping diffraction event is poorly resolved showing that aliasing can cause problems for the ALFT, even for irregularly sampled data. For Figure 14, a variable spatial bandwidth, as a function of frequency, was used. For lower frequencies this avoids the higher wavenumbers to be estimated in the ALFT.

Finally, in Figure 15, the anti-alias ALFT is used. This effectively combines the advantage of an adaptive bandwidth reduction for lower frequencies with a further de-aliasing of the higher frequencies, in particular. The (probably aliased) energy around a normalized wavenumber of 0.2 and frequency of 40 Hz is reduced, and the steeply dipping event has been reconstructed well.

A second field example is shown in Figures 16-21. Once again this is from a highly complex data area with multiple conflicting dips and aliased arrivals (particularly in the cross-line direction). Figure 16 shows an inline section on a nominal grid. The section in Figure 17 clearly indicates the aliasing problem in the cross-line direction. Figure 18 shows a cross-line of data, before interpolation and regularization to the desired fine output grid. The same cross-line is shown in Figure 19 after regularization with the anti-alias ALFT. Finally, Figures 20 and 21 show a second example before and after regularization with the anti-alias ALFT. This example is a section with strongly dipping diffractions, and includes events in the deeper section with poor S/N ratio. In both cases the anti-alias ALFT does a good job of reconstructing the data.

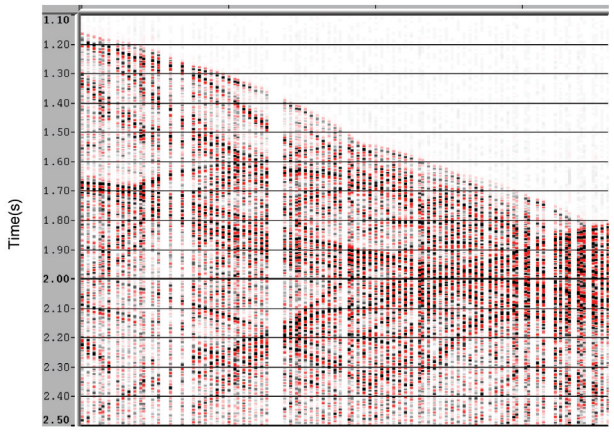

Figure 18 *The area of the cross-line section highlighted in Figure 17 on the desired fine output grid before regularization.*

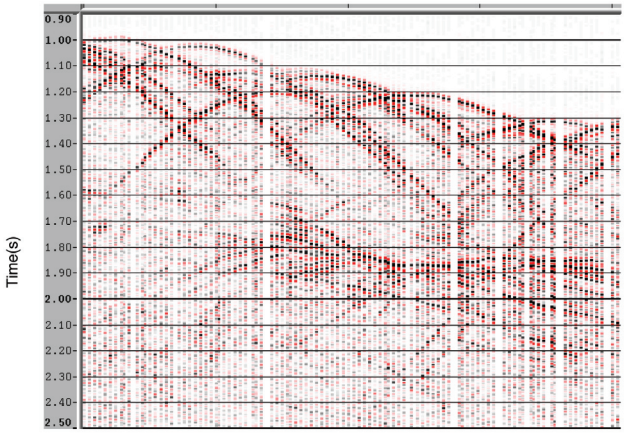

Figure 20 *A second example cross-line on the desired fine grid spacing before regularization.*

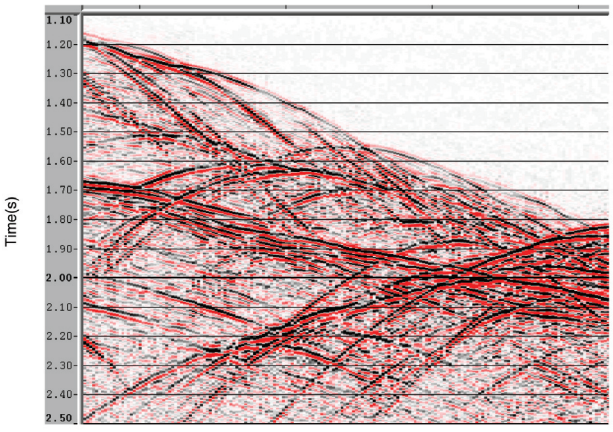

Figure 19 *The data in Figure 18 after regularization to the desired fine output grid using the anti-alias ALFT.*

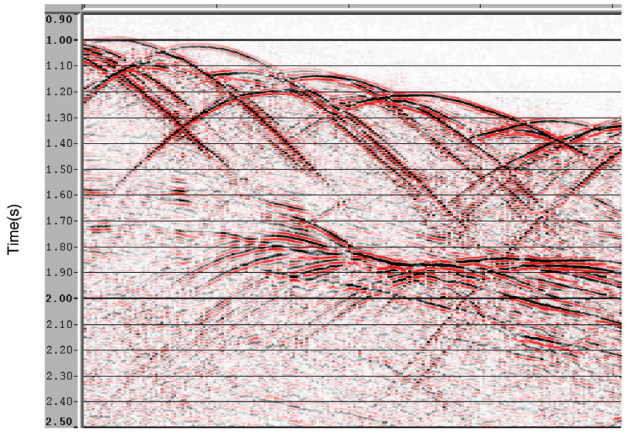

Figure 21 *The data in Figure 20 after regularization to the desired fine output grid using the anti-alias ALFT.*

Conclusion

The anti-alias ALFT uses un-aliased lower frequencies to provide spectral weights for the higher frequencies which can help to avoid the selection of aliased components in the ALFT. It is shown on 2D synthetic and 3D field data that the method can give a significantly better preservation of the higher frequencies for steeply dipping events.

Acknowledgements

PGS would like to thank Repsol for kind permission to use some of the data examples within this article.

References

Abma, R. and Kabir, N. [2006] 3D interpolation of irregular data with a POCS algorithm. *Geophysics*, **71**, 91-97.

Canning, A. and Gardner, G. H. F. [1996] Another look at the question of azimuth. *The Leading Edge*, **15**(7), 821-823.

Duijndam, A.L.W., Schonewille, M.A. and Hindriks, C.O.H. [1999] Reconstruction of band-limited signals, irregularly sampled along one spatial direction. *Geophysics*, **64**, 524-538.

Eiken, O., Waldemar, P., Schonewille, M., Haugen, G. U. and Duijndam, A. [1999] A proven concept for acquiring highly repeatable towed streamer seismic data. *61st EAGE Annual Meeting*, Session: 1040.

Liu, B., and Sacchi, M.D. [2004] Minimum weighted norm interpolation of seismic records. *Geophysics*, **69**, 1560-1568.

Sacchi, M.D. and Ulrych, T.J. [1996] Estimation of the discrete Fourier transform, a linear inversion approach. *Geophysics*, **61**, 1128-1136.

Schonewille, M., Klaedtke, A. and Vigner, A. [2009] Anti-alias anti-leakage Fourier transform. *79th SEG Annual Meeting*, Houston. Expanded Abstracts.

Xu, S., Zhang, Y., Pham, D.L. and Lambaré, G. [2004] On the orthogonality of anti-leakage Fourier transform based seismic trace interpolation. *74th SEG Annual Meeting*, Expanded Abstracts, 2013-2016.

Xu, S., Zhang, Y., Pham, D.L. and Lambaré, G. [2005] Antileakage Fourier transform for seismic data regularization. *Geophysics*, **70**, 87-95.

Zwartjes, P.M. and Sacchi, M.D. [2007] Fourier reconstruction of nonuniformly sampled, aliased seismic data. *Geophysics*, **72**, 21-32.